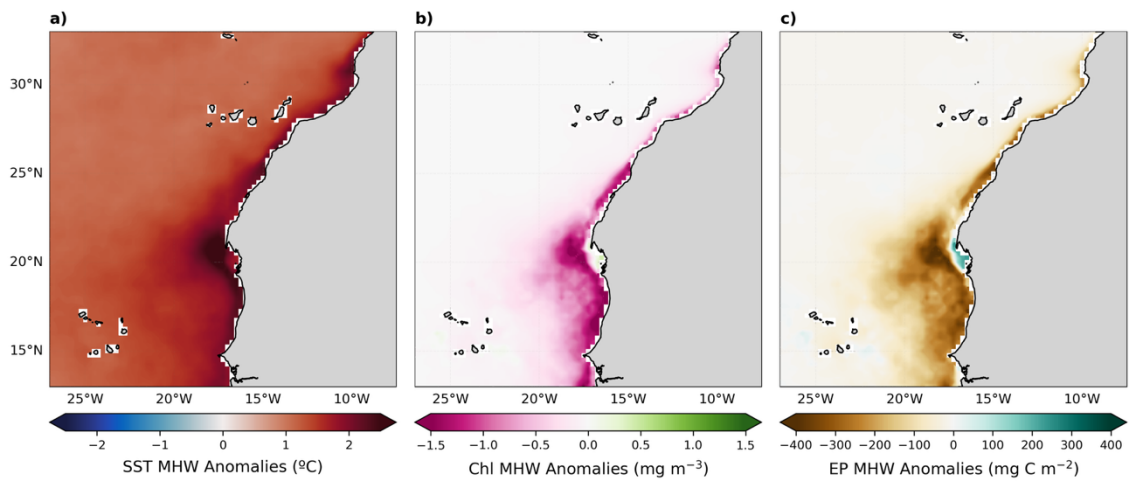
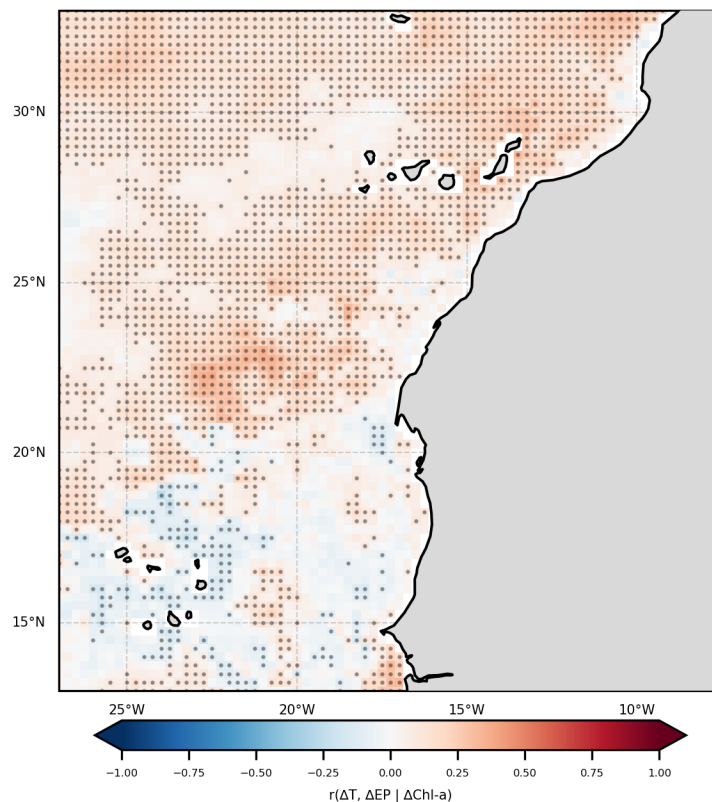


# 1 Supplementary Figures

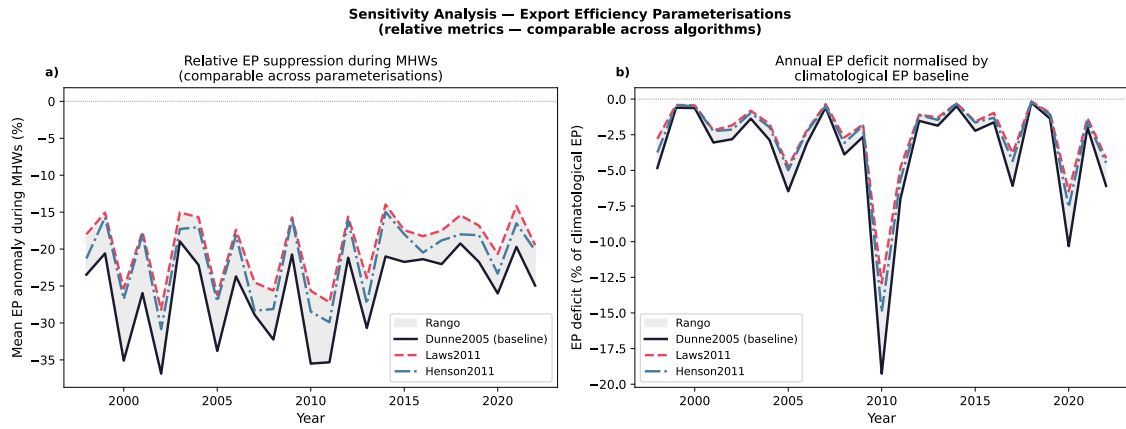


**Supplementary Figure 1: MHW influence on sea surface temperature, Chlorophyll-a concentration, and export production across the CanEBUS.** Composite mean anomalies during MHW days (1998–2022) for (a) sea surface temperature (SST; °C), (b) chlorophyll-a concentration (Chl-a;  $\text{mg m}^{-3}$ ), and (c) export production (EP;  $\text{mg C m}^{-2}$ ), computed relative to the climatological non-MHW days baseline. Positive SST anomalies exceeding  $+1^\circ\text{C}$  extend uniformly across the domain (a), co-occurring with widespread negative Chl-a anomalies concentrated along the coastal upwelling band (b). Consistently, EP anomalies are predominantly negative nearshore (c), suggesting MHWs translate into a substantial deficit in carbon export to depth.



**Supplementary Figure 2: Partial correlation between  $\Delta T$  and  $\Delta EP$  controlling for  $\Delta Chl-a$  across the CanEBUS during MHW events.** Pixelwise partial correlations  $r(\Delta T, \Delta EP | \Delta Chl-a)$  over the 1998–2022 period, isolating the direct thermal pathway on carbon export production after removing the linear effect of chlorophyll-a anomalies ( $\Delta Chl-a$ ). Stippling indicates grid cells where the partial correlation is statistically significant at the FDR-corrected  $p < 0.05$  level, with p-values computed using the effective sample size ( $N_{\text{eff}}$ ) to account for

17 temporal autocorrelation. The lack of a spatially coherent negative signal suggests that MHW-driven export  
 18 losses are unlikely to arise from an instantaneous direct thermal effect alone. Instead, the delayed EP response  
 19 documented in the lagged composites (Fig. 3) indicates that thermal extremes affect carbon export through  
 20 time-dependent upper-ocean restructuring and biological recovery processes.  
 21



22 **Supplementary Figure 3: Sensitivity of carbon export deficit to export efficiency parametrization.** (a) Time  
 23 series of mean relative export production (EP) anomaly during MHW days, computed as the pixelwise departure  
 24 from the daily climatological baseline expressed as percentage, averaged across all pixels with MHW. (b) Time  
 25 series of annual EP deficit normalized by the total climatological EP for each year. Three independent export  
 26 efficiency parametrizations were used: Dunne et al. (2005; baseline, solid black), Laws et al. (2011; dashed red),  
 27 and Henson et al. (2011; dash-dot blue). Grey shading indicates the inter-parametrization range.  
 28  
 29

Recovery window	Annual EP deficit (Tg C yr <sup>-1</sup> )	Amplification vs. MHW-only (%)	MHW thermal stress/Annual EP deficit (r <sup>2</sup> )	Southern Region fraction (%)
MHW days only (baseline)	6.15 ± 8.24	—	0.71	~62
1 day of positive EP anomaly	13.76 ± 13.78	~124	0.66	~68
3 consecutive days of positive EP anomaly	16.92 ± 16.78	~175	0.65	~68
5 consecutive days of positive EP anomaly	20.95 ± 19.14	~240	0.64	~67

30 **Supplementary Table 1: Sensitivity of annual carbon export deficit estimates to post-MHW recovery**  
 31 **window.** Annual carbon export production (EP) deficit, amplification factor relative to the MHW-days-only  
 32 baseline, coefficient of determination (r<sup>2</sup>) between annual MHW thermal stress and EP deficit, and fractional  
 33 contribution of the Southern Region (south of 21°N) to the total CanEBUS deficit, computed for recovery  
 34 windows of 1, 3, and 5 consecutive days of positive EP anomalies (ΔEP ≥ 0) following MHW termination. The 3-  
 35 day window was adopted as the default (Fig. 3i-l). Annual deficit values represent domain-integrated means ±  
 36 1 standard deviation over the 1998–2022 study period. Amplification is expressed relative to estimates based  
 37 exclusively on days formally classified as MHWs.  
 38